engineering proceedings

MDPI

Proceeding Paper

Microwave Radar Imaging as a Tool for Medical Diagnostics

Antonio Cuccaro [1], Angela Dell'Aversano[2], Bruno Basile[3], and Raffaele Solimene [2,4,*]

1 DIMES-University of Calabria, Rende (CS), Italy, antonio.cuccaro@unical.it (A.C.)
2 Dipartimento di Ingegneria, Università degli Studi della Campania Luigi Vanvitelli, 81031 Aversa, Italy; angela.dellaversano@gmail.com (A.D.A.), Raffaele Solimene (R.S.)
3 TTC Medical, Casalnuovo di Napoli, bruno.basile@temnografia.it (B. B.)
4 Consorzio Nazionale Interuniversitario per le Telecomunicazioni-CNIT, 43124 Parma, Italy
* Correspondence: raffaele.solimene@unicampania.it

Abstract: Microwave radar imaging is diagnostic technique that is receiving great attention in the research community for the potential striking advantages it may potentially offer. Nonetheless, to pursue the diagnostics by microwave radar imaging is extremely is difficult due to the theoretical as well as practical reasons. In this contribution, in particular, we focus on the need to take into account frequency dispersion effects and the antenna's frequency response. More in details, we propose an imaging algorithm that works by completely ignoring the tissue frequency behaviours as well as the antenna's response. Numerical results for simplified breast layout obtained by a full-wave electromagnetic solver confirms the potentiality of the proposed approach.

Keywords: Microwave radar imaging; medical diagnostics; breast cancer detection.

1. Introduction

Breast cancer is the most frequent cause of death due to cancer among female patients [1,2]. In this framework, early detection is crucial since the survival rate depends on the stage the disease is when it is diagnosed [3,4]. That is why, scholars continue to focus on the improvement of currently employed diagnostic methods as well as on the development of new imaging modalities that can supplement the first ones. In the last decades, microwave breast imaging (MBI) was the subject of a great deal of research since it does not rely on ionizing radiations, does not require breast compression and the related technology is relatively cheap [5]. Moreover, MBI is sensitive to the dielectric contrast between the normal and diseased tissues, which in turn is generally higher than the radiographic density contrast [6]. Results show in literature suggest that MBI can actually be used for breast cancer [7–9].

Many algorithms for MBI have been developed [10] till now. Some of them directly reconstruct the 3D scenario under test, others, instead, reconstruct the scene as a collections of 2D problems (sliced approach), which reduces the imaging algorithm complexity [11]. In general, microwave breast imaging entails solving a non-linear ill-posed inverse scattering problem which is much more difficult than for X-ray tomography since diffraction phenomena cannot be ignored. Non-linear inversions are cast as an optimization problem where the misfit between the measured and the model data is generally minimized by iterative algorithms [12]. Accordingly, the related reconstruction procedures are computationally heavy [13] and can be trapped in some false solutions [14]. Assuming a linear scattering model simplifies the imaging problem and leads to the so-called radar imaging approach [15]. In this case, the imaging is robust against noise and uncertainties and computationally effective, though the corresponding images appear more like hot maps where strong inhomogeneities are detected. Eventually, the radar imaging allows for only the detection and the localization of targets which have a strong dielectric contrast with respect to the surrounding background tissues. The beam-forming (BF) algorithm is for sure the most

check for updates

Citation: Cuccaro, A.; Dell'Aversano, A.; Basile, B.; Solimene, R. Microwave Radar Imaging for Breast Cancer Detection. *Eng. Proc.* **2023**, *1*, 0. https://doi.org/

Published:

Copyright: © 2023 by the authors. Licensee MDPI, Basel, Switzerland. This article is an open access article distributed under the terms and conditions of the Creative Commons Attribution (CC BY) license (https://creativecommons.org/licenses/by/4.0/).

popular MBI method. Basically, for each pixel in the scene, the received signals are properly time-shifting and the summed so to focus at the considered pixel belonging to the spatial area to be imaged [16]. Different variant of BF have been proposed in literature, [17–19]. A detailed analytical study on the achievable performance by BF methods has been reported in [20], where the working frequency and the number of spatial data points, was highlighted.

Even under the simplified framework of the radar approach, to success in the imaging a number of issues need to be properly dealt with. For example, before imaging, data must be pre-processed in order to reduce the clutter due to the antenna's internal reflection, the skin interface and other non-tumor breast tissues [21]. Another important issue to face is the frequency dispersion of breast tissues. This is particularly true for wide band imaging methods and because the tissues generally vary from patient to patient. Also, the antenna antenna frequency response is hard to predict since it works in close proximity to breast and therefore, is actually unknown [22,23].

In this contribution, we assume that the background measurement is available so that the focus on the issue related to the tissue frequency dispersion and antenna's frequency response. It is clear that these two issues entail performance degradation in standard BF methods. This is mainly because standard BF "coherently" combine data collected at different frequencies. Indeed, frequency dispersion and unknown antenna's response lead to error while devising the delay set to be used in the beam-forming procedure. To mitigate such a drawback, in this contribution we extend the results reported in [22,24,25], by employing a non-coherent BF imaging strategies. In particular, we shown that the performance are satisfactory although, during the imaging stage, the antenna's frequency response is completely ignored and the tissue variations with frequency are not accounted for. To this end, differently from [26,28], we perform a numerical analysis but consider a 3D reconstruction procedure (instead of the sliced approach used in [26]) and a multistatic configuration.

2. Measurement configuration description

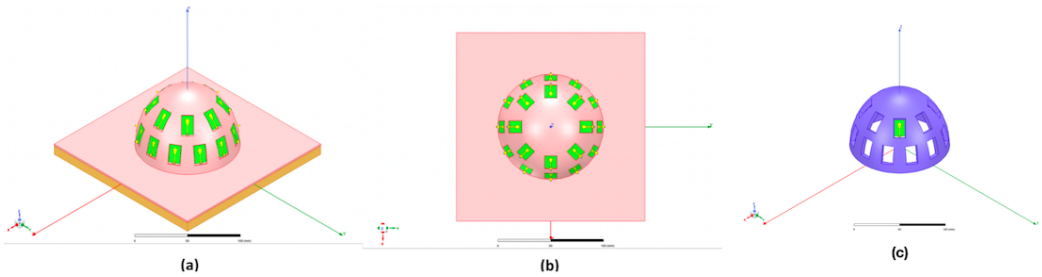

Figure 1. Measurement configuration: in (a) and (b) two views with $N = 20$ slot antennas are arranged over a hemispherical cup which hosts the breast under test, in (c) picture of hemispherical cup in absence of the breast

Let N antennas be located over a surface that surrounds the breast under test. Denote as $\underline{r}_{on}$, for $n = 1, 2, \cdots, N$, the positions of the corresponding antenna phase centers. The antennas are actually arranged over a hemispherical cup as sketched in Fig. 1 (a)(b). This solution offers a number of advantages. First, the system has not sliding antennas. This makes the acquisition quicker and there are no mechanical transients to wait for before staring data collection. Second, the locations of the antennas with respect to the breast are precisely known. This is because when the breast is inserted in the cup the latter shapes the breast so to conform to the cap surface. Of course, this requires cups of different sizes since breasts are different. In this contribution, the cup has internal radius of 50mm. Finally, the material of the cup can be suitably selected in order to improve the matching between the antenna and the breast. In particular, acrylonitrile butadiene styrene (ABS) material is used and the cup has N=20 empty housings where to place the antennas (Fig.1(c)). This, along

with a proper design of the antennas, allows to avoid the use of the coupling medium, which is, instead, commonly employed in microwave breast imaging systems. As to the antennas, we consider printed slot dipoles built on FR4 substrate of thickness 0.8mm (see Fig. 1(c)). More in detail, the antennas are designed to work in direct contact to the breast within $[4, 6]$ GHz frequency band. This way, the breast loads the antenna so that miniaturization can be achieved. In particular, the antennas are designed while in contact to a breast numerical phantom consisting of only skin and fat layers. This is reasonable since skin and fat always are the first tissues electromagnetic waves need to propagate through. Also, for antenna design, the skin and fat layers are considered planar and having thicknesses 1.5 mm and 50 mm, respectively. This speeds up the antenna optimization process while using a full-wave electromagnetic solvers. As to the electromagnetic properties, we employed the four-poles Cole-Cole models reported in [27], which at the central frequency (i.e., 5 GHz in our case) gives 35.78 and 5.08 for the relative dielectric permittivity of the two tissues and 3.06 S/m and 0.24 S/m for the conductivity of the skin and fat, respectively. Note that, these are nominal values that can be in general different from the actual ones.

The size of each single antenna turns to be 18 mm x 11 mm, so that N=20 antennas can easily be arranged over the cup. The positions (sketched in Fig. 1(a)(b)) are chosen so to have a good coverage of the breast during the irradiation stage. Generally, to improve the matching between the antenna and the breast to investigate a coupling medium is adopted. Our system this could be achieved by adopting a thin dielectric layer (i.e. $\lambda/4$, where λ is the wavelength evaluates to the central frequency band) corresponding at the antenna housings so that the antenna are not directly in contact to the breast. However, by adopting slot antennas that work in direct contact to the breast, both miniaturization and good coupling can be achieved without coupling media.

3. Imaging algorithm

The imaging problems consists in obtaining an image of the scene of the target under test from scattering measurements. The most commonly employed measurement configuration is the monostatic one for which the scattered field is collected only in correspondence of the transmitting antennas. Herein, instead, we consider a multistatic configuration. Hence, while one antenna is transmitting, the field data are collected over the whole set of deployed antennas. Then, the process is repeated for each antenna. According, up two N^2 measurements are available for each employed frequency.

To perform the reconstructions we first need to establish the math model whose inversion is actually the reconstruction process. To this end, we refer to the following equation

$$S(\omega, \underline{r}_{on}, \underline{r}_{om}) = S_{nm}(\omega) = (j\omega/2\pi v)\tilde{P}(\omega) \int_D \frac{\exp\left[\frac{-j\omega}{v}(|\underline{r}_{on} - \underline{r}| + |\underline{r}_{om} - \underline{r}|)\right]}{|\underline{r}_{on} - \underline{r}||\underline{r}_{om} - \underline{r}|} \chi(\underline{r}) d\underline{r}, \quad (1)$$

where $S_{nm}(\omega)$ is the scattering measurement at the angular frequency ω when the m-th antenna acts as transmitter and the n-th one as receiver, D is the spatial region under investigation and v the background medium propagation speed. Moreover, $\tilde{P}(\omega) = H_r(\omega)P(\omega)H_t(\omega)$, with $H_r(\omega)$ and $H_t(\omega)$ being the receiving and transmitting antenna frequency responses and $P(\omega)$ the Fourier spectrum of the transmitted pulse. Finally, $\chi(\underline{r})$ is the so-called contrast function which describes the target in terms of its dielectric relative difference with respect to the background medium.

Equation (1) relies on different assumptions. First, the scattering phenomenon is considered being linear by invoking the Born approximation [29,30]. The cost to pay, as argued in the introduction, is that the corresponding images allow only to highlight and locate strong inhomogeneities. Also, the propagation speed is assumed known and constant. Although linearization hardly works and constant velocity clearly does not

comply with the typical inhomogeneous and unknown tissue distribution of the breast, these assumptions are actually behind any radar imaging approach.

In (1), $H_r(\omega), H_t(\omega)$ and $P(\omega)$ are assumed known as well. However, since the antennas are located closely, or even in contact, to the breast, which in turn is unknown, these quantities are unknown too. Therefore, classical beam-forming algorithms can experience a significant performance degradation. To see this, look at the BF indicator reported below (see [20])

$$I_{BF}(\underline{r}) = \left| \int_{\Omega} \sum_{n=1}^{N} \sum_{m=1}^{N} S_{nm}(\omega) \exp\left[j\omega\tau_{nm}(\underline{r})\right] d\omega \right|^2, \tag{2}$$

where Ω is the frequency band, $\underline{r}$ is the focusing point and $\tau_{nm}(\underline{r}) = (|\underline{r}_{on} - \underline{r}| + |\underline{r}_{om} - \underline{r}|)/v$ the set of delays to achieve focusing. Since $H_r(\omega), H_t(\omega)$ and $P(\omega)$ shape the data frequency behaviour, it is mandatory to have their precise estimations. This, however, is difficult due to the close proximity set up. It must be emphasized that this drawback arises because the frequency data are coherently summed. To mitigate this problem we propose incoherent beam-forming (IBF) strategy. The related indicator is reported below,

$$I_{IBF}(\underline{r}) = \int_{\Omega} \left| \sum_{n=1}^{N} \sum_{m=1}^{N} S_{nm}(\omega) \exp\left[j\omega\tau_{nm}(\underline{r})\right] \right|^2 d\omega, \tag{3}$$

where the basic difference with respect to (2) is clearly that data are summed in amplitude along the frequency domain. From the achievable performance point of view, in [20] it was shown that, for a monostatic configuration, the main difference occurs in the side-lobe of the point-spread function, hence the achievable resolution are practically the same in both cases. The same is expected to hold for the considered multistatic configuration.

4. Some numerical results

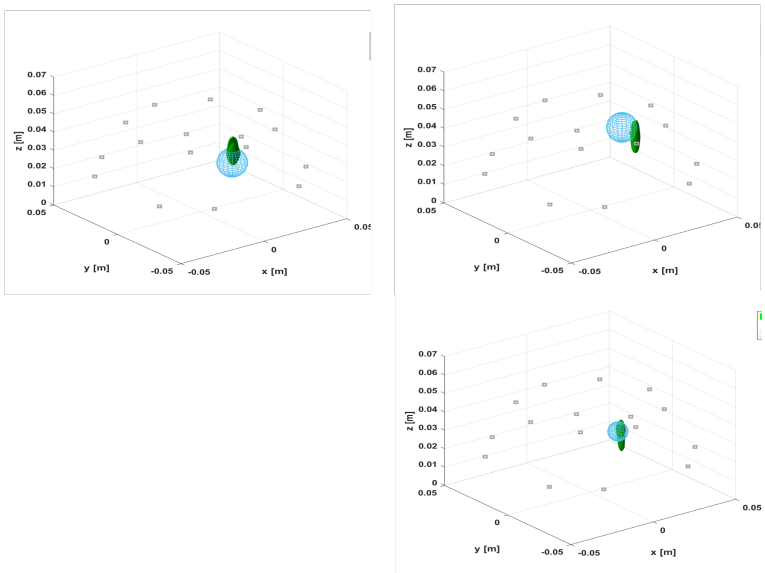

Figure 2. Reconstructions obtained via (3). The blue spheres represent the actual tumours, the green patches the corresponding reconstructions and the white squares denote the antenna positions. The reconstructions on the first row refers to the tumour's radius of 10 mm whereas the reconstruction on the second row to the radius of 5 mm.

To show the effectiveness of the proposed imaging procedure, in this section we present some numerical examples. In particular, the result refers to the case the breast consists of only skin and fat with features randomly perturbed 10% with respect to the nominal values mentioned above. The tumour is represented by a spherical inhomogeneity

with diameter of 10 mm or 5 mm and three cases corresponding to different positions inside the breast are considered. Finally, in the reconstruction process the background medium velocity is set equal to the one in the nominal fat tissue. The reconstruction results are reported in Fig. 2. As can be seen, the tumour is clearly detected and localized.

5. Conclusions

Microwave breast imaging is a promising diagnostic method that can be used to help standard imaging modalities. Nonetheless, to the successful, MBI requires to properly address a number of issues. In this contribution, we just spotted the light on the one related to the antenna's response. The antenna's response has to be accounted for during the imaging stage since it "shapes" the actually received pulse and, above all, modifies the overall round-trip delay. This requires that it must be estimated so to allow to be put in or compensated for. Because in diagnostics the antennas are generally deployed in close proximity, or even in contact, to the target under test (in this paper we considered the breast), the antenna couples with the unknown target. As a consequence, its response deviates from its free-space counterpart. Therefore, while the latter can be easily measured/estimated, it shows to be of less practical use in diagnostics. This inconvenient is exacerbated by the patient to patient tissue changes. In this paper, we have shown that the knowledge of the antenna's frequency response is not necessarily required. Indeed, we have shown that the related issue can completely be overcome by processing each frequency data separately and then by incoherently combining the single-frequency images. The presented results, though refer to a simplified scenario, are satisfactory and encourage the development of a more in depth study by accounting more realistic breasts.

Author Contributions: conceptualization, B.B. and R.S.; methodology, A.C., A.D. and R.S., A.C.; software, A.C. and A.D.; validation, A.C., A.D.; formal analysis, A.C. and A.D.; writing original draft preparation, A.C., A.D. and R.S.; supervision, R.S.. All authors have read and agreed to the published version of the manuscript.

Funding: This research was funded by B&B under the contract "ATTIVITA' DI RICERCA E PROGETTAZIONE DI DISPOSITIVI DI DETECTION A RADIOFREQUENZA PER DEVICE DI DIAGNOSTICA MEDICA PER IL SENO - RIFERIMENTO PROGETTO MIT MEDICAL DEVICE – AVVISO PUBBLICO PER IL SOSTEGNO ALLE MPMI CAMPANE CUP B17H22001730007".

Institutional Review Board Statement: Not applicable.

Acknowledgments: Antonio Cuccaro acknowledges the MUR (Ministero dell'Università e della Ricerca), Italy, as part of Project PNRR "AGE-IT" (Ageing well in an ageing society) a valere sull'avviso Partenariati Estesi (PE) del MUR.

Conflicts of Interest: The authors declare no conflict of interest.

References

1. Ferlay, J.; Soerjomataram, I.; Eser, R.D.S.; Mathers, C.; Rebelo, M.; Parkin, D.M.; Forman, D.; Bray, F. Cancer incidence and mortality worldwide: sources, methods and major patterns in GLOBOCAN 2012. *Int. J. Cancer* **2015**, *136*, E359–E386.
2. Levi, F.; Bosetti, C.; Lucchini, F.; Negri, E.; La Vecchia, C. Monitoring the decrease in breast cancer mortality in Europe. *Eur. J. Cancer Prev.* **2005**, *14*, 497–502.
3. Myers, E.R.; Moorman, P.; Gierisch, J.M.; Havrilesky, L.J.; Grimm, L.J.; Ghate, S.; Davidson, B.; Mongtomery, B.R.C.; Crowley, M.J.; McCrory, D.C.; et al. Benefits and Harms of Breast Cancer Screening: A Systematic Review. *JAMA* **2015**, *314*, 1615–1634.
4. Siegel, R.L.; Miller, K.D.; Jemal, A. Cancer statistics. *CA Cancer J. Clin.* **2016**, *66*, 7–30.
5. Preece, A.W.; Craddock, I.; Shere, M.; Jones, L.; Winton, H.L. Maria M4: Clinical evaluation of a prototype ultrawideband radar scanner for breast cancer detection. *J. Med. Imaging* **2016**, *3*, 033502-1–033502-7.
6. Meaney, P.M.; Fanning, M.W.; Li, D.; Poplack, S.P.; and Paulsen, K.D. A clinical prototype for active microwave imaging of the breast. *IEEE Trans. Microw. Theory Tech.* **2000**, *48*, pp. 1841–1853.
7. O'Loughlin, D.; O'Halloran, M.; Moloney, B.M.; Glavin, M.; Jones, E.; Elahi, M.A. Microwave Breast Imaging: Clinical Advances and Remaining Challenges. *IEEE Trans. Biomed. Eng.* **2018**, *65*, 2580–2590.
8. Kwon, S.; Lee, S. Recent Advances in Microwave Imaging for Breast Cancer Detection. *Int. J. Biomed. Imaging* **2016**, 5054–5912.
9. Larsen, L.; Jacobi, J. Microwaves offer promise as imaging modality. *Diagn. Imaging* **1982**, *11*, 44–47.
10. Nikolova, N.K. Microwave imaging for breast cancer. *IEEE Microw. Mag.* **2011**, *12*, 78–94.

11. Golnabi, A.H.; Meaney, P.M.; Epstein, N.R.; Paulsen, K.D. Microwave imaging for breast cancer detection: Advances in three-dimensional image reconstruction. In Proceedings of the 2011 Annual International Conference of the IEEE Engineering in Medicine and Biology Society, Boston, MA, USA, 30 August–3 September 2011; pp. 5730–5733.
12. Wang, L. Early Diagnosis of Breast Cancer. *Sensors* **2017**, *17*, 1572.
13. Donelli, M.; Craddock, I.; Gibbins, D.; Sarafianou, M. A three-dimensional time domain microwave imaging method for breast cancer detection based on an evolutionary algorithm. *Prog. Electromagn. Res. M* **2011**, *18*, 179–195.
14. Isernia, T.; Pascazio, V.; Pierri, R. On the local minima in a tomographic imaging technique. *IEEE Trans. Geosci. Rem. Sens.* **2001**, *39*, 1596–1607.
15. Chew, W.C. *Waves and Fields in Inhomogeneous Media*; IEEE Press: New York 1995.
16. Chen, J.; Yao, K.; Hudson, R. Source localization and beamforming. *IEEE Signal Process. Mag.* **2002**, *19*, 30–39.
17. Hagness, S.C.; Taove, A.; Bridges, J.E. Two-dimensional FDTD analysis of a pulsed microwave confocal system for breast cancer detection: Fixed focus and antenna array sensors. *IEEE Trans. Biomed. Eng.* **1998**, *45*, 1470–1479.
18. Lim, H.; Nhung, N.; Li, E.; Thang, N. Confocal microwave imaging for breast cancer detection: delay-multiply-and-sum image reconstruction algorithm. *IEEE Trans. Biomed. Eng.* **2008**, *55*, 1697–1704.
19. Klemm, M.; Craddock, I.J.; Leendertz, J.A.; Preece, A.; Benjamin, R. Improved delay-and-sum beamforming algorithm for breast cancer detection. *Int. J. Ant. Propag.* **2008**.
20. Solimene, R.; Cuccaro, A.; Ruvio, G.; Tapia, D.F.; Halloran, M.O. Beamforming and Holography Image Formation Methods: An Analytic Study. *Opt. Express* **2016**, *24*, 9077–9093
21. Ruvio, G.; Solimene, R.; Cuccaro, A.; Fiaschetti, G.; Fagan, A.J.; Cournane, S.; Cooke, J.; Ammann, M.J.; Tobon, J.; Browne, J.E. Multimodal Breast Phantoms for Microwave, Ultrasound, Mammography, Magnetic Resonance and Computed Tomography Imaging. *Sensors* **2020**, *20*, 2400.
22. Ruvio, G.; Solimene, R.; D'Alterio, A.; Ammann, M.J.; Pierri, R. RF breast cancer detection employing a non-characterized vivaldi antenna and a MUSIC-like algorithm. *Int. J. RF Microw. Comput. Aided Eng.* **2013**, *23*, 598–609.
23. Ruvio, G.; Cuccaro, A.; Solimene, R.; Brancaccio, A.; Basile, B.; Ammann, M.J. Microwave bone imaging: A preliminary scanning system for proof-of-concept. *IEEE Healthc. Technol. Lett.* **2016**, *3*, 218–221.
24. Ruvio, G.; Solimene, R.; Cuccaro, A.; Ammann, M.J. Comparison of Non-Coherent Linear Breast Cancer Detection Algorithms Applied to a 2-D Numerical Breast Model. *IEEE Antennas Wirel. Propag. Lett.* **2013**, *41*, 853–856.
25. Ruvio, G.; Solimene, R.; Cuccaro, A.; Gaetano, D.; Browne, J.E.; Amman, M.J. Breast cancer detection using interferometric MUSIC: Experimental and numerical assessment. *Med. Phys.* **2014**, *41*, 102101–102111.
26. Cuccaro, A.; Dell'Aversano, A.; Ruvio, G.; Browne, J.E.; Solimene, R. Incoherent radar imaging for breast cancer detection and experimental validation against 3D multimodal breast phantoms. *J. Imaging* **2019**, *7*, 23.
27. Gabriel, S.; Lau, R.W.; Gabriel, C. Dielectric properties of biological tissue: III. Parametric models for the dielectric spectrum of tissues. *Phys. Med. Biol.* **1996**, 41, 2271-2293.
28. Solimene, R.; Basile, B.; Browne, J.; Cuccaro, A.; Dell'Aversano, A.; Ruvio, G. An incoherent radar imaging system for medical applications. In Proceedings of the 2021 IEEE Conference on Antenna Measurements and Applications (CAMA), Antibes Juan-les-Pins, France, 15-17 November 2021.
29. Marengo, E. A.; Galagarza, E. S., Solimene, R. Data-driven linearizing approach in inverse scattering. *J. Opt. Spc. Am. A* **2017**, *34*, 1561–1576.
30. Solimene, R.; Buonanno, A.; Soldovieri, F.; Pierri, R. Physical optics imaging of 3-D PEC objects: Vector and multipolarized approaches. *IEEE Trans. Geoscience Rem. Sens.* **2009** *48*, 1799–1808.